Optimal design of the Integrated Modular Power Electronics Cabinet

Xavier Giraud, Marc Budinger, Xavier Roboam, Hubert Piquet, Marc Sartor, Jérôme Faucher

Optimal design of the Integrated Modular Power Electronics Cabinet

X.Giraud (1,2,3), M.Budinger (2), X.Roboam (3), H.Piquet (3), M.Sartor (2), J.Faucher (1)

1 : Airbus Operations SAS, 316 route de Bayonne, 31060 Toulouse Cedex 9, France
2 : Université de Toulouse, ICA (INSA, UPS, Mines Albi, ISAE), 135 av.de Rangueil, 31077 Toulouse, France
3 : Université de Toulouse, LAPLACE (CNRS/INPT/UPS), 2 Rue Camichel, 31071, Toulouse, France

Abstract : *This paper deals with a new concept of electrical power distribution system called IMPEC for Integrated Modular Power Electronics Cabinet. The paper defines methods aiming at carrying out an optimal design of IMPEC, the main variables being on one hand the number and size of power electronics module. On the other hand, reconfigurations between these modules and electrical loads are also optimized.The formalization of the problem highlights that designers must deal simultaneously with a combinatorial explosion and a multi-physical system sizing. The main objective of the study is to propose a methodological framework for solving this original optimal design problem. A heuristic-based algorithm is developed to solve this combinatorial optimization problem. A particular attention is paid to develop a weight estimation procedure using generic sizing models. Finally a mapping is performed to identify the best solutions and to highlight the technological components having the most significant sensitivity on the complete system weight.*

Keywords : more electrical aircraft, power electronics, optimal design, multi-physical sizing, combinatorial optimization

Nomenclature

APU	Auxiliary Power Unit	IMA	Integrated Modular Avionics
DOE	Design Of Experiments	IMPEC	Integrated Modular Power Electronics Cabinet
DSM	Design Structure Matrix	MEA	More Electrical Aircraft
ECS	Environmental Control System	N2D	N-square Diagram
EPS	Electrical Power System	PEM	Power Electronics Module
HVDC	High Voltage Direct Current	WIPS	Wing Ice Protection System

$\mathcal{C}$	Total number of loading cases to analyze
$I_{PEM,max}$	Maximum PEM current
$\mathcal{L}$	Total number of IMPEC electrical loads to supply
MAT_{min}	Minimal Contactor Matrix
N_{Sol}	Number of possible reconfiguration solution of the contactor matrix
n_x	Number of x (see below to have the values)
θ	Organic solution
$\tilde{p}_l^c$	Power demand of the load « l » in the loading case « c »
W_S	Total weight of the system IMPEC
W_x	Weight of x (see below to have the values)
$z_{l,m}^c$	Connexion of the PEM « m » to the load « l » in the loading case « c »
Z	Reconfiguration solution

Possible values of the indice x:

PEM	Power Electronics Module	ct	Contactor
L	Inductance	cha	Power center chassis
C	Capacitor	cp	Cold plate
hx	Heat exchanger		

I. Introduction and context

I.1 More Electrical Aircraft

On traditional aircraft such as A320 or A330, systems are powered by 3 different energy vectors: pneumatic, hydraulic and electric (Figure 1 and Figure 2). These 3 power vectors are extracted from primary power sources such as the engines or the auxiliary power unit (APU) that are today all supplied by fuel (kerosene) [1].

In terms of power levels, the pneumatic vector is the most demanding one. During some flight phases, it represents around 80% of the power taken off the engines (Figure 1). This energy vector supplies the engine starting system, the wing anti-ice protection system (WIPS) as well as the environment control system (ECS) by extracting pressurized air taken from the engines (bleed air).

Systems requiring high force at low speed such as flight control surface actuation, landing gear actuation and aircraft breaking are traditionally powered by the hydraulic vector.

Eventually, the electrical power system (EPS) provides power to numerous and various systems (also called electrical loads). On-board an Airbus A330, around 700 electrical loads are embedded. Some of them are essential such as: the fuel pumps, the electro-hydraulic pumps, the fans, the processing blades ; others are installed in order to provide comfort to the passengers: the galleys and the flight-entertainment systems.

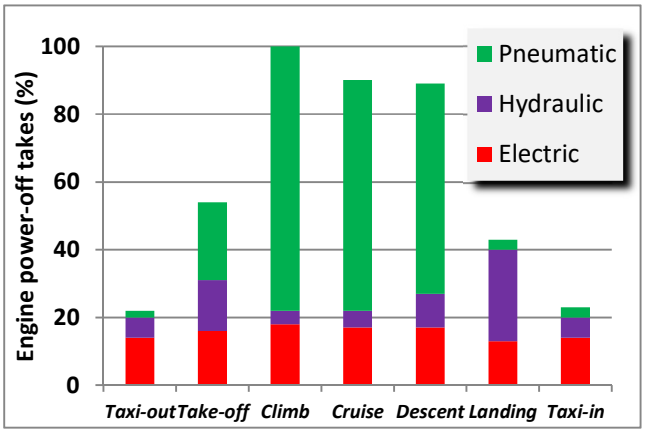

Figure 1 Sharing of the power-off take extracted from the engines (Airbus A330) [2]

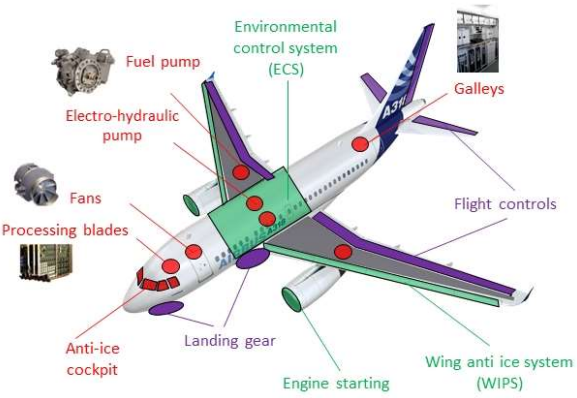

Figure 2 Physical implementation of main power consuming systems on traditional aircraft

For the last decade, the use of electricity is rapidly increasing in commercial aircraft. This trend illustrated in the paradigm of the More Electrical Aircraft (MEA) consists in replacing hydraulic and/or pneumatic powered systems by electrical ones [3] [4] [5]. As a consequence, the realization of the "all-electrical" aircraft aims at completing simultaneously 2 types of configurations: Bleedless [6] and Hydraulicless [7] [8] (Figure 3). By embedding only 2 hydraulic circuits instead of 3 traditionally, the Airbus A380 and A350 are seen as an intermediate configuration towards hydraulicless aircraft [9]. On the other side, the Boeing 787 is a complete bleedless aircraft by supplying electrically: the ECS, the WIPS and the engine starting [6].

Today, the MEA is seen as a major axis of improvement for the aviation industry to achieve increasingly ambitious objectives: decrease of weight, rationalization of costs, reducing environmental impact... In this frame, several research projects are today launched in order to progress on architecture and technology axis [10] [11].

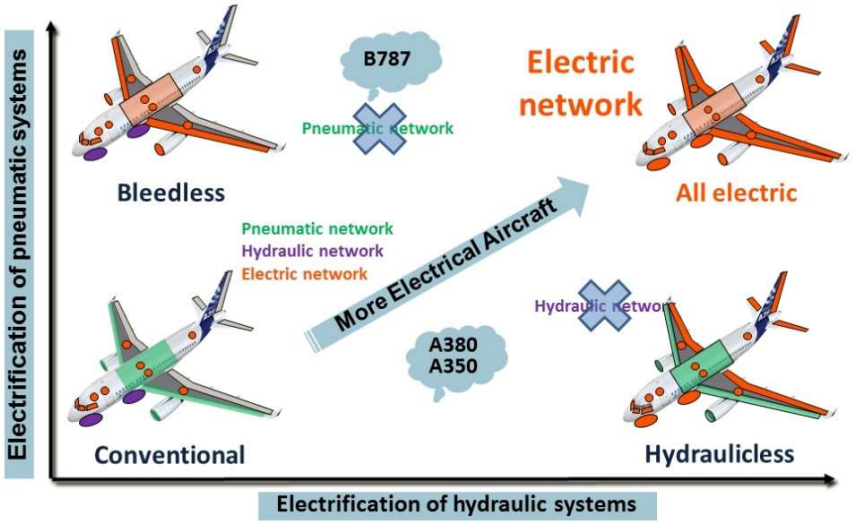

Figure 3 The 2 axis of the more electrical aircraft (MEA)

I.2 High demanding loads requiring power electronics in bleedless configuration

In terms of power demand, the bleedless aircraft configuration is the most challenging one. It is often said that the bleedless effect leads to multiply by 4 the electrical power generation [4]. For instance, the Boeing 787 comprises 4 generators of 250 kVA whereas a bigger aircraft such as the Airbus A380 "only" embeds 4 generators of 150 kVA.

The ECS is the main contributor of the power step change. The ECS electrification requires installing electrical air compressors consisting of permanent magnet synchronous motors driven by power electronics modules (i.e inverter). The compressors can consume up to 100 kW during some operational cases. As the consequence, the bleedless effect will lead to a significant increase of the power amount transmitted by the power electronics modules (PEM).

I.3 Classical use of power electronics in aeronautics

On today aircraft, an electrical machine is supplied by a dedicated PEM often located close to the actuator. Depending on the voltage levels provided by the EPS, two structures appear (Figure 4) :

- When the load is allocated to an AC busbar (Figure 4-A), a rectifying stage is required to create a local HVDC bus (+/- 270 VDC).
- When HVDC busbars are provided by the EPS (Figure 4-B), the rectifier stage is removed and the PEM is directly connected to a HVDC busbar.

These two structures where each load has its dedicated PEM have 3 major drawbacks:

- **Reliability aspect**. The PEM loss leads inevitably to the load loss. This aspects can have an impact on the availability/reliability of the aircraft function carried out by the load.
- **Cost aspect**. Each PEM is sized by its load. On the Figure 4 example, two different PEM sizes are required: 40 kW and 75 kW. This leads to an increase of the amount of equipment references also called *"part numbers"*. This list of equipment shall be as low as possible in order to increase standardization and reduce costs. Of course, it would be possible to have only one PEM reference of 75 kW but this would lead to an oversizing and therefore a weight increase.

- **Utilization rate**. A given set of loads or aircraft functions are only supplied during a reduced period of the mission. For example, these 3 systems are not active during the same operational case: the *engine starting*, the *landing gear actuation* and the *engine thrust reversers*…Electrifying each system with one PEM each could lead to a low PEM utilization rate.

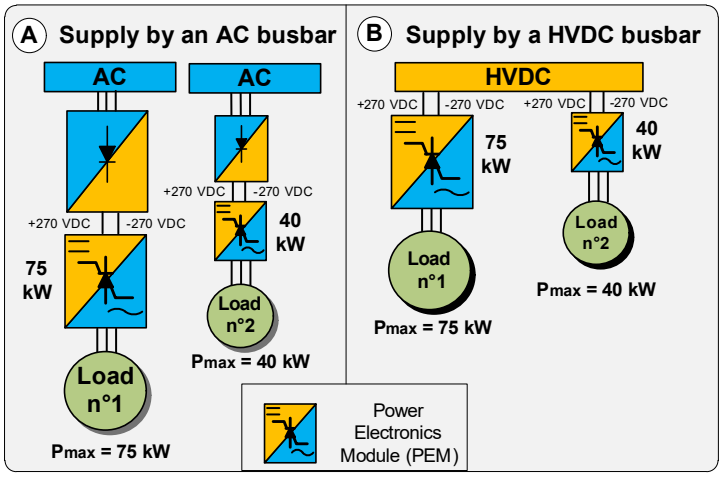

Figure 4 Two classical structures to supply an electrical machine

I.4 Non-simultaneous power demand peaks for the MEA

The analysis of the power demand of most consuming loads for the MEA, such as the ECS electrical air compressors, show important fluctuations during the flight mission. This trend is illustrated by the Figure 5 showing that the power demand profiles are different from one load to another : the respective load power demand peaks appear in different flight phases. For example, the maximum power demand of the ECS load n°1 appears in the flight phases n°1, 2, 4 and 21 (ground phases) whereas the ECS load n°2 work a full power during the phases n°5 and 20.

The IMPEC structure aims at facing this issue by mutualizing standardized PEMs between different consumers in various flight phases.

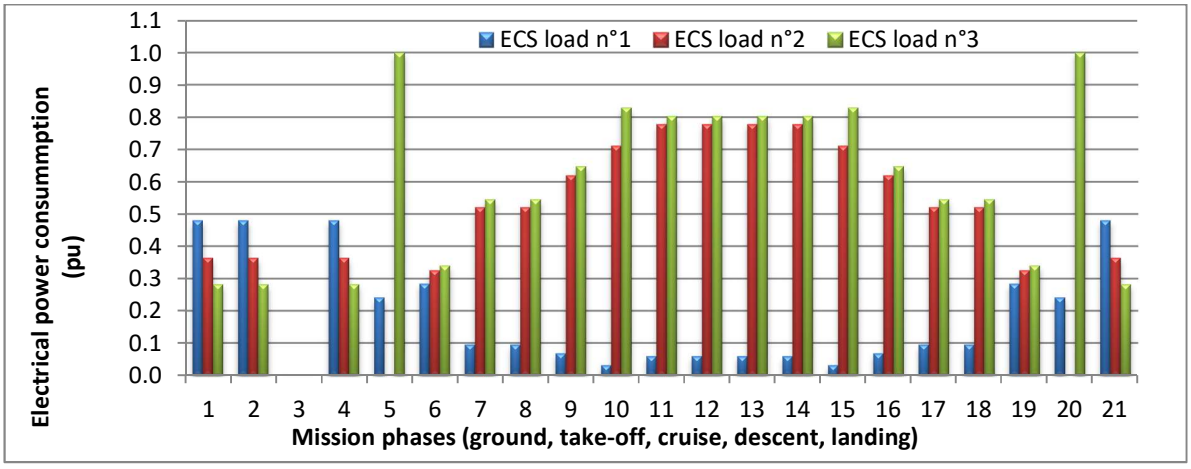

Figure 5 Power demand of the 3 electrical air compressors according to the aircraft mission phases

I.5 Paper structure

In the general context presented here before, the present paper is organized into 6 parts:

- the *section n°2* describes the IMPEC concept being the system under study in this paper. The IMPEC organic structure is presented as well as the advantages of this new power distribution concept.
- the *section n°3* is dedicated to the presentation of the optimization problem associated to the IMPEC optimal design. The two main sources of problem complexity are identified and illustrated with examples.
- the *section n°4* aims at providing an overview of the sizing procedure deriving the overall system weight and features of IMPEC implementations.
- the *section n°5* presents the optimization algorithm developed to solve the optimal design problem.
- the *section n°6* is a post-optimal analysis aiming to identify the most robust solution forms and the component technology sensitivities on the overall system weight.

II. The IMPEC concept

In aeronautics, a new concept enabling to supply several loads requiring an inverter is under study. IMPEC concept stands for Integrated Modular Power Electronics Cabinet [12]. It is made of an electrical power center hosting a set of PEMs that have the same features (modularity/standardization) and that can supply several loads included in the power center perimeter (mutualisation).

II.1 State of the art on modularity and mutualisation of electronics in aircraft

Modularity and mutualisation of electronics embedded in Airbus aircraft are only implemented for processing electronics. On conventional aircraft (e.g A320), each system has one or several processing blades covering its own calculation need. With the A380 launched in the mid-2000, the IMA concept (Integrated Modular Avionics) has been implemented in order to minimize the number of equipment references (*part numbers*) [13] [14] . The main benefits expected from this concept are cost and reliability. The IMA consists of a set of standardized processing blades and a communication network ensuring the data transmission. An important mutualisation is achieved since one processing blade can host applications coming from different systems.

Mutualisation of power electronics is a relatively new concept in aeronautics and more generally in the industrial fields linked to electrical engineering. Two types of mutualisation can be highlighted:

1) A first one consists in **using a same PEM to supply different loads at different instants according to the operational needs**. This is today applied for the Bleedless aircraft Boeing 787. One PEM (called MCU for Motor Control Unit in Figure 6) ensures the engine starting [4]. Once the engines are running, the same PEM supplies the ECS electrical compressor for the rest of the mission. Thus, the same PEM supplies two different systems: “Engine starting” and “ECS”.

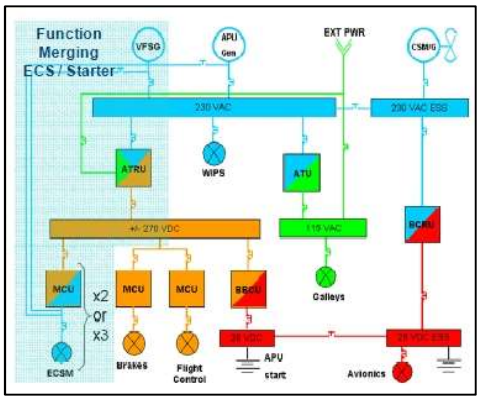

Figure 6 Simplified schematics for the Boeing B787 electrical network

2) A second type of mutualisation **consists in associating several PEMs together in order to supply a same load**. This concept, introduced in [12], enables to obtain different levels of electrical production capacities. For instance, with 4 PEMs of 30 kW each, it is possible to form four different power levels: 30, 60, 90 and 120 kW. An additional flexibility is therefore obtained in order to stick as much as possible to the operational needs of the electrical consumers.

II.2 IMPEC features

II.2.1 Architecture and operation modes

IMPEC implements the 2 types of mutualisation concepts presented here before. The IMPEC structure is made of 2 main parts: **a set of modular PEMs** (all being identical) providing power through HVDC bus and **a contactor matrix** ensuring the connexions between the PEM and the loads. In comparison with the IMA, the *processing blades* are the PEMs and the *contactor matrix* plays the role of the communication network. The main functioning principles are the following ones:

- One PEM can only supply one load at the same time;
- One PEM can supply different loads during the flight mission: it can supply one load during the "take-off" phase and another load during the "cruise" phase;
- One load can be supplied by one or several PEMs at the same time (PEM paralleling);

The Figure 7 shows a principle example of an IMPEC implementation made of 4 PEMs of 30 kW each. An example of the contactor matrix configuration is shown for a case during which all the PEMs are available (right side of Figure 7).

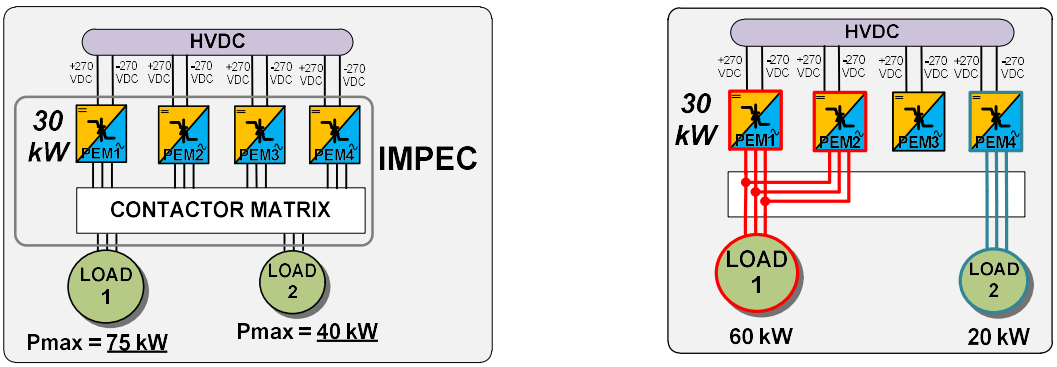

Figure 7 Structure of an IMPEC implementation (on the left) – Example of configuration of the contactor matrix with loads n°1 and n°2 consuming respectively 60 and 20 kW (on the right)

II.2.2 IMPEC components and architecture

The Figure 8 shows the organic architecture of an IMPEC implementation made of only 2 PEMs. According to the power paths formed by the contactors, the 2 PEMs supply 1 load each. In more details, the physical structure of the IMPEC is the following one:

- PEMs made of 3 devices: an inverter part based on IGBT modules (component n°**1** of Figure 8), a cold plate (**2**) and a DC link capacitor (**3**).
- Single phase inductances (**4**) at the output of each PEM leg. These inductances are not part of the standardized PEM. They are mandatory for the PEM mutualisation (i.e PEM paralleling). Thus, a PEM which is never put in parallel with another PEM will not require having output inductances.
- A contactor matrix (**5**) ensuring necessary connexions between modules and loads. A contactor ensures the connexion between one module and one load. As shown on the Figure 8, the closure of the "contactor 1-2" connects the PEM 1 to the load 2.
- A power center chassis (**6**) integrating mechanically all the components listed here before.
- A heat exchanger (**7**) evacuating the heat extracted by the cold plates.

As it will be explained in the section III, the definition of the commutation components (the inductances and the contactor matrix) is strongly impacted by the IMPEC reconfiguration represented by the different connections : module/load.

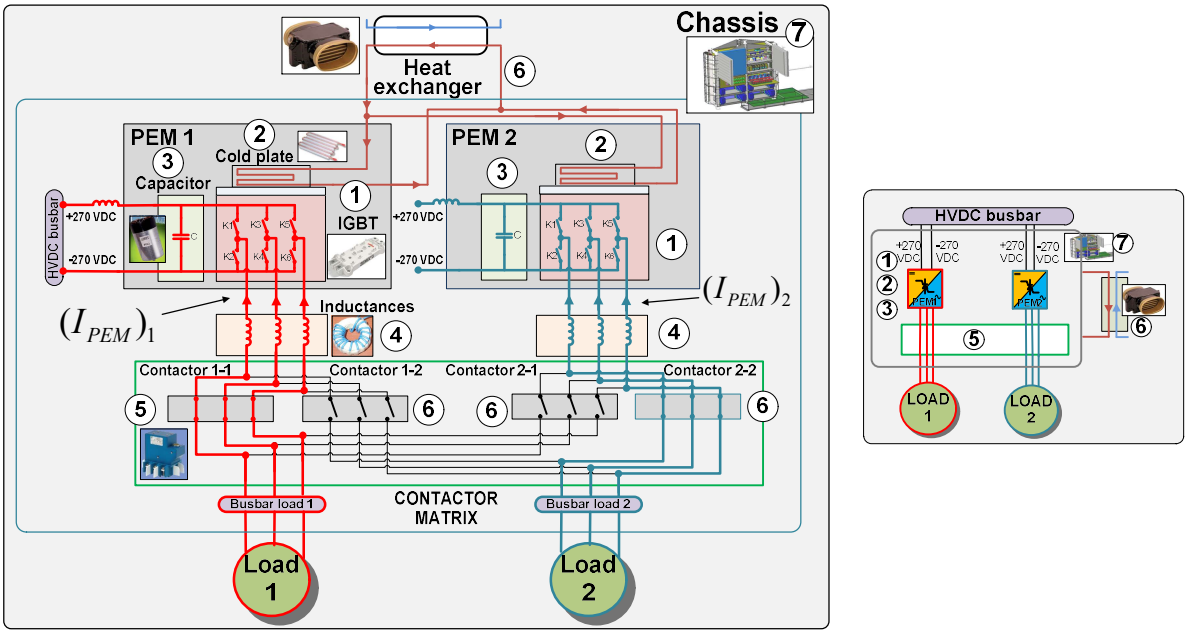

Figure 8 Left side : electrical schematic view of two PEM supplying one load each / Right side : functional view of this PEM-load association

II.2.3 IMPEC advantage n°1: robustness against PEM failures

Depending on the number of contactors installed in the contactor matrix, it is possible to connect any load to any PEM. With IMPEC, the loss of one PEM does not lead to a load loss whereas it is the case with a classical structure (each load has its dedicated PEM).

On the Figure 9, this feature is illustrated by the examples on which two different PEM loss configuration are highlighted. As shown on the Figure 7 (right), in the nominal configuration, the load n°1 is supplied by the PEM1 & 2 and the load n°2 by the PEM4. When there is a failure of the PEM2, the PEM3 takes over the supply of the load n°1. When this is only the PEM4 which is inoperative, the load n°2 is still supplied thanks to the PEM3.

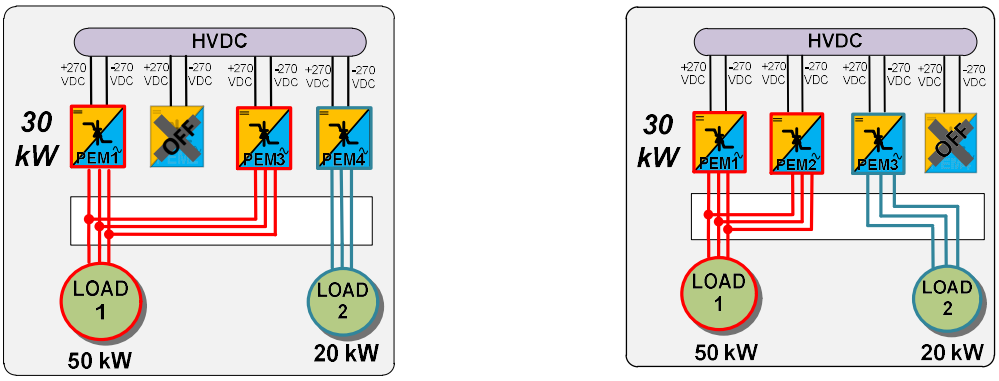

Figure 9 Examples of contactor matrix configuration for different PEM losses

II.2.4 IMPEC advantage n°2 : flexibility according to power demands

The contactor matrix offers the possibility to have better matching between the PEMs use during the flight mission and the power demand fluctuations of the loads. This capability is illustrated by the example showing two cases (Figure 10). In the case n°1, the load n°1 and n°2 are consuming respectively 75 kW and 30 kW: 3 PEMs are then required for the load n°1 and only 1 PEM for the load n°2. When the load n°2 consumes its maximum power (40 kW) in the case n°2, both PEM3 and PEM4 are required. The PEM3 has been "freed" by the load n°1 because its consumption has decreased in comparison with the case n°1.

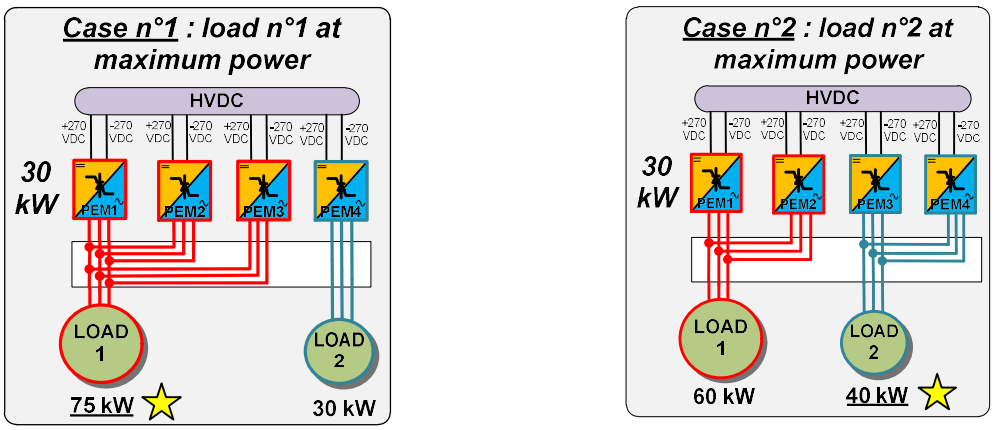

Figure 10 Reconfiguration of the contactor matrix in order to fit with the load power demands

II.3 Studied use case and requirements

All the design methods developed in this paper are applied and tested on an industrial use case with a bleedless aircraft configuration. As shown on the Figure 11, IMPEC shall supply 6 different electrical loads: 3 electrical air compressors of the environmental control system (loads: ECS1, ECS2, ECS3), 1 electrical pump for the fuel tank inerting system (load: FTIS), 1 load modelling the cabin systems supplied by the IMPEC (load: CS) and 1 load representing the electrical motor ensuring the engine starting (load : ENG START). As depicted by the Figure 11, the number of PEMs is not assumed, being a degree of freedom for

system design. The value of this variable will be part of the optimization process in order to reach an optimal solution in terms of IMPEC system weight.

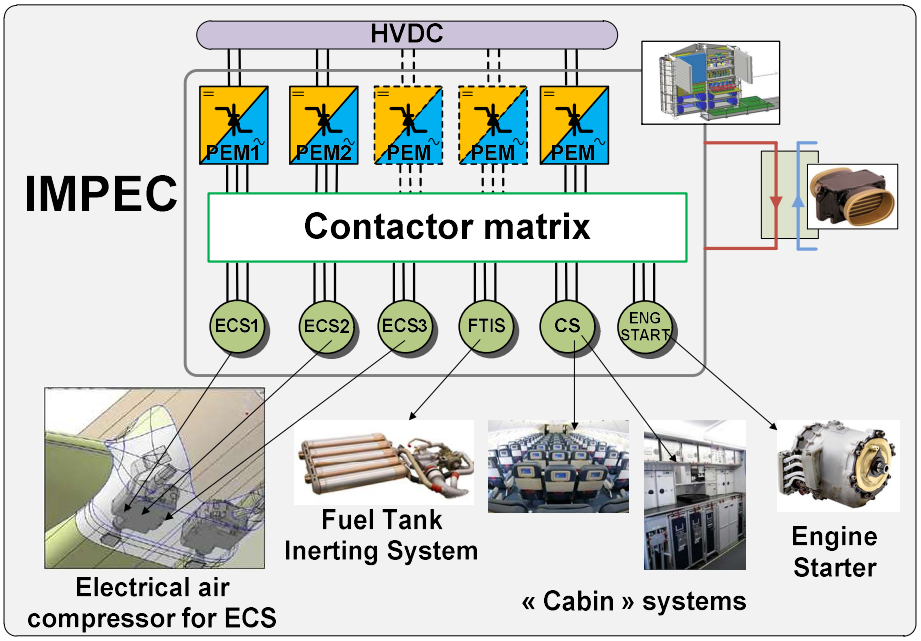

Figure 11 Use case for the assessment of the optimization design methods

III. Optimal design problem

III.1 Optimal design problem formulation

III.1.1 Design variables

The optimal design problem comprises 2 types of decision variables:

- the number of PEMs (modules) « n_{PEM} » ;
- the reconfiguration solution defining all the connections *load/module* for all the operational cases. A reconfiguration solution is modeled by the 3-dimension matrix « Z » storing the binary variables « $z_{l,m}^{c}$ ». These variables are defined as follows:

$$\forall\, m \in \{1,..,n_{PEM}\},\quad \forall\, l \in \{1,..,\mathcal{L}\},\quad \forall\, c \in \{1,..,\mathcal{C}\},\qquad z_{l,m}^{c} = \begin{cases} 1, \text{load "}l\text{" is connected to the PEM "}m\text{" for the case "}c \\ 0, \text{otherwise} \end{cases} \qquad Eq\ 1$$

Where « $\mathcal{L}$ » is the number of loads to be supplied by IMPEC, and « $\mathcal{C}$ » is the number of loading cases to be considered for the design. The loading cases represent all the operational cases that shall to be taken into account in the design [15]. A loading case is defined by 4 dimensions :

- a *flight phase* (e.g take-off);
- a *mode of the IMPEC electrical system* (e.g loss of 2 PEMs);
- a *mode of the other systems* (e.g loss of one ECS electrical compressor);
- an *external condition* (e.g hot day).

As one dimension can have many values (for example, 21 flight phases are considered), several thousands of loading cases « C » are considered for the industrial use case.

The use of the 2 design variables introduced here before is illustrated by an example displayed on the Figure 12. The IMPEC structure is made of « $n_{PEM} = 5$ ». The reconfiguration solution « Z » is graphically represented by a parallelepiped. The configuration of the loading case n°1 « $c = 1$ » is highlighted.

Eventually, it must be noted that according to this configuration of the case n°1, at least 5 contactors are required between : L1-PEM1 ; L2-PEM3 ; L3-PEM2 ; L4-PEM4 ; L4-PEM5. In addition, as PEM4 and PEM5 are in parallel to supply the FTIS load, inductances are required at the outputs of both PEMs.

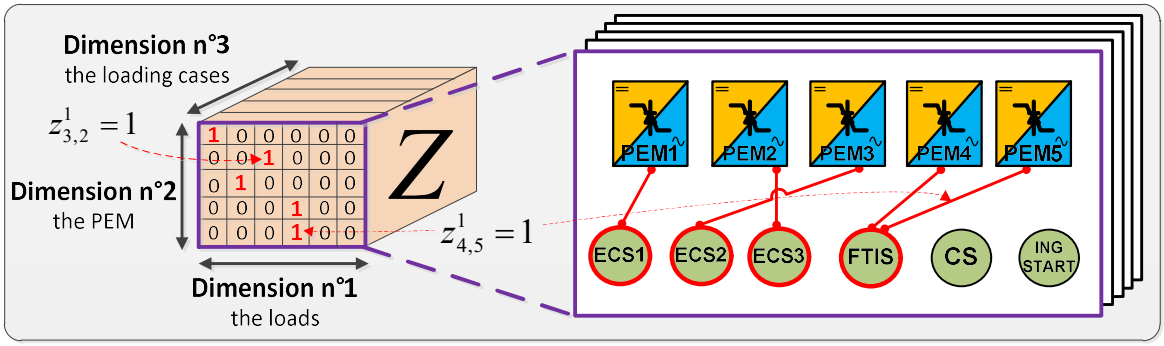

Figure 12 Graphical representation of the design variables with a selected configuration for the loading case n°1

III.1.2 Design objective

As very often in the aeronautics industry, the design objective consists in minimizing the overall weight of the system. This is here modelled by:

$$F = \min(W_S) = \min(n_{PEM}.W_{PEM} + n_L.W_L + n_{ct}.W_{ct} + W_{cha} + W_{hx}) \qquad Eq\ 2$$

Where « W_S » is the overall IMPEC system weight, « n_{PEM} » and « W_{PEM} » are respectively the number of PEMs and their weight; « n_L » and « W_L » are respectively the number of inductances and their weight ; « n_{ct} » and « W_{ct} » are respectively the number of contactors and their weight ; « W_{cha} » is the chassis weight and « W_{hx} » is the heat exchanger weight.

In order to reduce the number of "*part numbers*" and to push the standardization as far as possible, all components of the same type have the same reference (i.e the same features: dimensions, weight). It means that there is one reference for : the IGBT modules, the capacitors, the cold plates, the inductances and the contactors.

With a view to differentiate the organic constitution of a solution and its management/control, an IMPEC solution « s » is defined by the couple « $s = (\theta, Z)$ » where :

- « θ » defines the physical constitution of the solution : the number of PEMs « n_{PEM} », the number of inductances « n_L », the number of contactors « n_{ct} », etc.
- « Z » represents the reconfiguration solution defined in the part III.1.

III.1.3 Design constraints

The first design constraint imposes that a consuming load shall be supplied and therefore connected to one available PEM:

$$\forall \{l,c\} \in \{1,..,\mathcal{L}\} \times \{1,..,\mathcal{C}\}, \quad if \;\; \tilde{p}_l^c > 0 \;\; then \;\; \sum_{m=1}^{n_{PEM}} z_{l,m}^c \geq 1 \qquad Eq\ 3$$

Where « $\tilde{p}_l^c$ » is the power demand of the load « l » in the loading case « c ». The dual constraint specifies that a PEM shall not be connected to a non-consuming load.

A second constraint specifies that one PEM supplies only one load in a given loading case:

$$\forall \{m,c\} \in \{1,..,n_{PEM}\} \times \{1,..,\mathcal{C}\}, \quad \sum_{l=1}^{\mathcal{L}} z_{l,m}^c \leq 1 \qquad Eq\ 4$$

The last main constraint consists in verifying that the power demand of one load does not exceed the power capacity of the PEM(s) connected to it. In terms of current, this is formulated by the following equation:

$$\forall \{c,l\} \in \{1,..,\mathcal{C}\} \times \{1,.,\mathcal{L}\},, \quad \sum_{m=1}^{n_{PEM}} z_{l,m}^c . I_{PEM,max} \geq \tilde{i}_l^c \qquad Eq\ 5$$

III.2 Two sources of complexity

III.2.1 Complexity source n°1 : a multi-physical system design

As highlighted in the Figure 13, the IMPEC architecture mixes components that shall be designed by considering different physical fields. For example, IGBT modules shall be defined by considering simultaneously thermal and electrical aspects. Moreover interactions exist between the different component size. For instance, the design decisions on the cold plate (e.g the fluid flow rate) will have an impact on the IGBT cooling as well as on the heat exchanger.

This problem complexity requires applying a systemic approach by considering all devices and corresponding physical fields as a whole. According to the perimeter and objectives of the study, the integrated models shall have the "right" level of details, being "just enough accurate" due the complexity of the optimal design process. This methodology developed to cope with problem complexity is presented in the part IV of this paper.

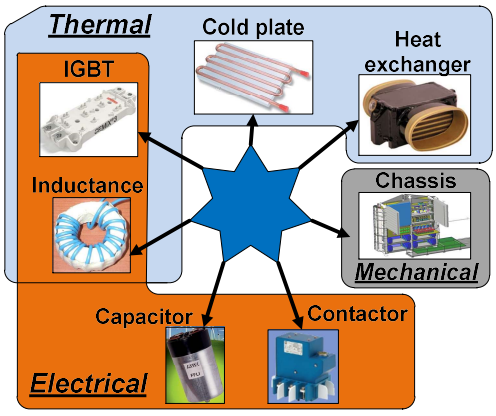

Figure 13 Main IMPEC components with identification the main physical fields

III.2.2 Complexity source n°2 : a combinatorial explosion for the contactor matrix reconfiguration

The « $z_{l,m}^{c}$ » values (*Eq 1)* shall be decided in order to define a reconfiguration solution « Z ». The number of possibilities is very high. Let us take a reduced-size example having the following features : « $n_{PEM} = 3$ », « $\mathcal{C} = 4$ », « $\mathcal{L} = 2$ ». The Figure 14 shows all the matrix contactor possibilities for each loading case (the number of parallelized PEMs is limited to 2). There are 12 matrix contactor choices for the case n°1; 2 for the cases n°2 and 3; 6 choices for the case n°4. In a graphical way, the reconfiguration problematic consists in selecting one square for each case. The combination of the squares form a reconfiguration solution. On the Figure 14, 2 different examples « $Z1$ » et « $Z2$ » are colored (green and purple).

Any combination of configurations leads to a reconfiguration solution. Thus the size of the design space is set by 2 features : the number of cases « $\mathcal{C}$ » and the number of potential contactor configuration per case « $(n_{conf})^{c}$ ». The total number of different reconfiguration solutions « Z », assessing the combinatorial space, is given by:

$$N_{sol} = \prod_{c=1}^{\mathcal{C}} (n_{conf})^{c} \qquad \textit{Eq 6}$$

Applying this formula, the total solution number of the Figure 14 example is: $12 \times 2 \times 2 \times 6 = 288$. For a problem having 5 consuming loads and 6 available PEMs, the number of potential matrix configurations for one case is : « $(n_{conf})^{c} = 2520$ ». For a problem made of 50 loading cases (still not in line with several thousand loading cases mentioned in the section III.1.1), the total number of reconfiguration solutions is given by:

$$N_{sol} = 2520^{50} \approx 10^{170} \qquad \textit{Eq. 7}$$

This simple example shows the highly combinatorial feature of the matrix reconfiguration problem. A combinatorial optimization approach is required in order to handle this complexity: an algorithm dedicated for the IMPEC application is presented in the section V.

Note: it is interesting to notice that this combinatorial explosion is also encountered by the other aircraft shared resource system: the IMA [13]. As a consequence the IMA optimal design also requires to build methodologies based on the use of combinatorial optimization algorithms [16].

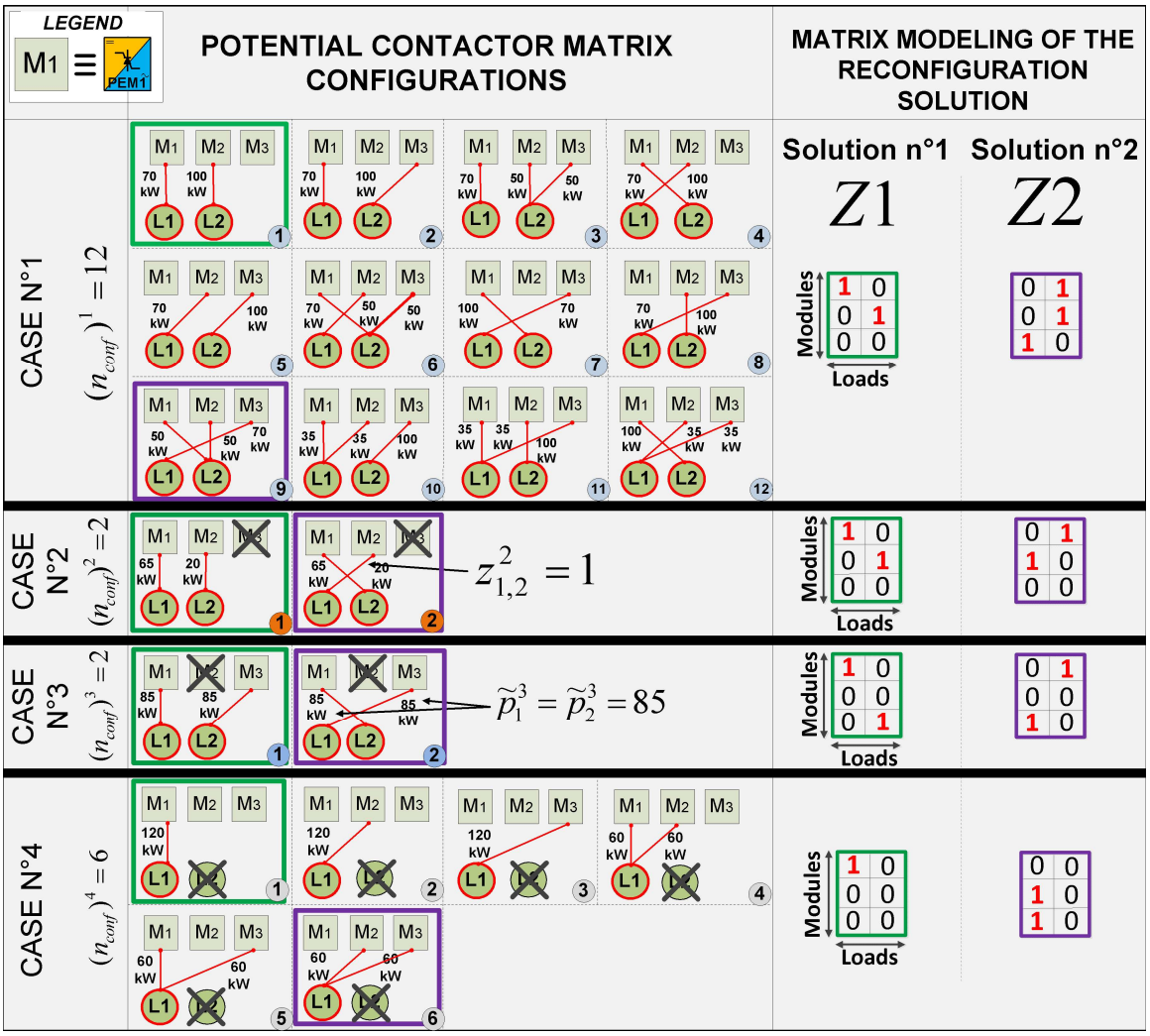

Figure 14 Potential contactor matrix configurations for each loading case and highlighting of 2 reconfiguration solutions

IV. Evaluation function : multi-physical sizing process

The multi-physical sizing process aims to compute a relevant system weight « W_S » according to the two design variables « n_{PEM} » and « Z ». As displayed on the Figure 15, a modular design methodology is intended to be developed by cutting the sizing process into different component blocks. Each block aims to design one component type: IGBT module, cold plate, etc. Two important axis are worked in order to have a computation-efficient sizing process with regards to high combinatorial aspect of the IMPEC optimal design problem:

- **Axis 1**: the sizing process organization: *what is the "less expensive" calculation sequence and the interactions (inputs/outputs) between the different blocks?*
- **Axis 2** : the sizing models: *what are the methods and the hypothesis to be applied in order to compute the main features of components?*

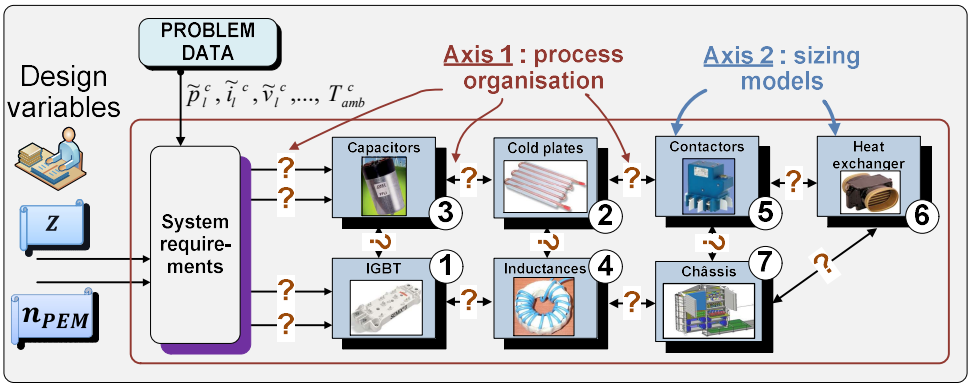

Figure 15 Highlighting of the sizing process problematic

IV.1 Axis 1 : the sizing process organisation

IV.1.1 State of the art

There are several different technics aiming to help the designer to organize a process. The formalisms can be different but they always manipulate generic notions:

- A decomposition of the process by **entities** ;
- A description of the **interactions or interdependencies** between these entities.

The causal diagram is a graphical representation in which each entity is modelled by a block and the interactions are identified by oriented arrows. This formalism was used to organize the sizing process of a flight control actuator [17]. On a causal diagram, it may be difficult to rapidly visualize the couplings between the different entities. They can be automatically detected either by a dedicated tool [18] or by formalizing the process using another type of diagram : the N-square Diagram (N2D) [19].

As the causal diagram does, a N2D models a process by a set of entities (blocks) and interactions (arrows). But the N2D introduces a graphical convention in order to have a better visualization of the block interactions : inputs are vertical arrows and outputs are horizontal arrows (Figure 16). Thanks to this formalism, the coupling of the Figure 16 example can be rapidly identified : between block 2 and 3 through the parameter 3 and 4.

The causal diagram and N2D can be mathematically represented by a Design Structure Matrix (DSM) [20]. The modelling is made by an adjacency matrix in which each entity is a column and a line. Thanks to the matrix formalism automated computation treatments can be applied [21].

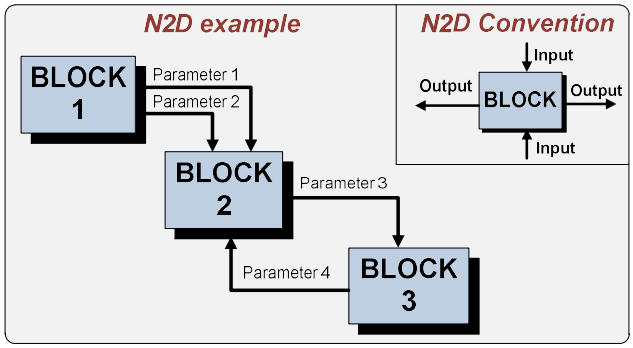

Figure 16 Input/output block convention for a N2D and N2D example made of several blocks

IV.1.2 IMPEC sizing process organization

The N2D formalism was chosen in order to model the sizing process organization (Figure 17). This diagram enables to visualize the calculation sequence. 7 blocks represent the sizing model of the different component types (IGBT module, cold plate,…). 4 types of information flows interact around these blocks:

- The **design hypothesis** belonging to different physical domains (e.g electrical domain with the switching frequency « F_{sw} » or thermal domain for the maximum IGBT junction temperature « $T_{j,max}$ »).
- The **system requirements.** According to the design variables « n_{MD} » and « Z » and the problem data (power demand of the loads « $\tilde{p}_l^c$ », the ambient temperature « T_{amb}^c »,…), system requirements are computed such as : the number of PEMs « n_{PEM} », the number of contactors « n_{ct} », the number of inductances « n_L », the voltage and currents delivered by each module during each case « $(V_{IGBT}, I_{IGBT})_m^c$ », « $I_{IGBT,max}$ » represents the maximum current seen by the IGBT switches and « $I_{L,max}$ » defines the maximum current flowing through the inductances. These system requirements are inputs for the different blocks.
- **Unitary weight** of the components.
- **Intermediate calculations** of component features. They are calculated by the associated component blocks but the features are injected into other blocks. For example, the IGBT current rating is derived by the "IGBT block" ant it is provided to the "Inductances block".

The algebraic cycles implying several components are broken by the introduction of the **design hypothesis**. The N2D formalism clearly shows that the sizing process can be calculated in a sequential way. There is no data feedback below the diagonal which would generate algebraic loops. This important feature enables to decrease significantly the computation routine time assessing the system weight « W_s ».

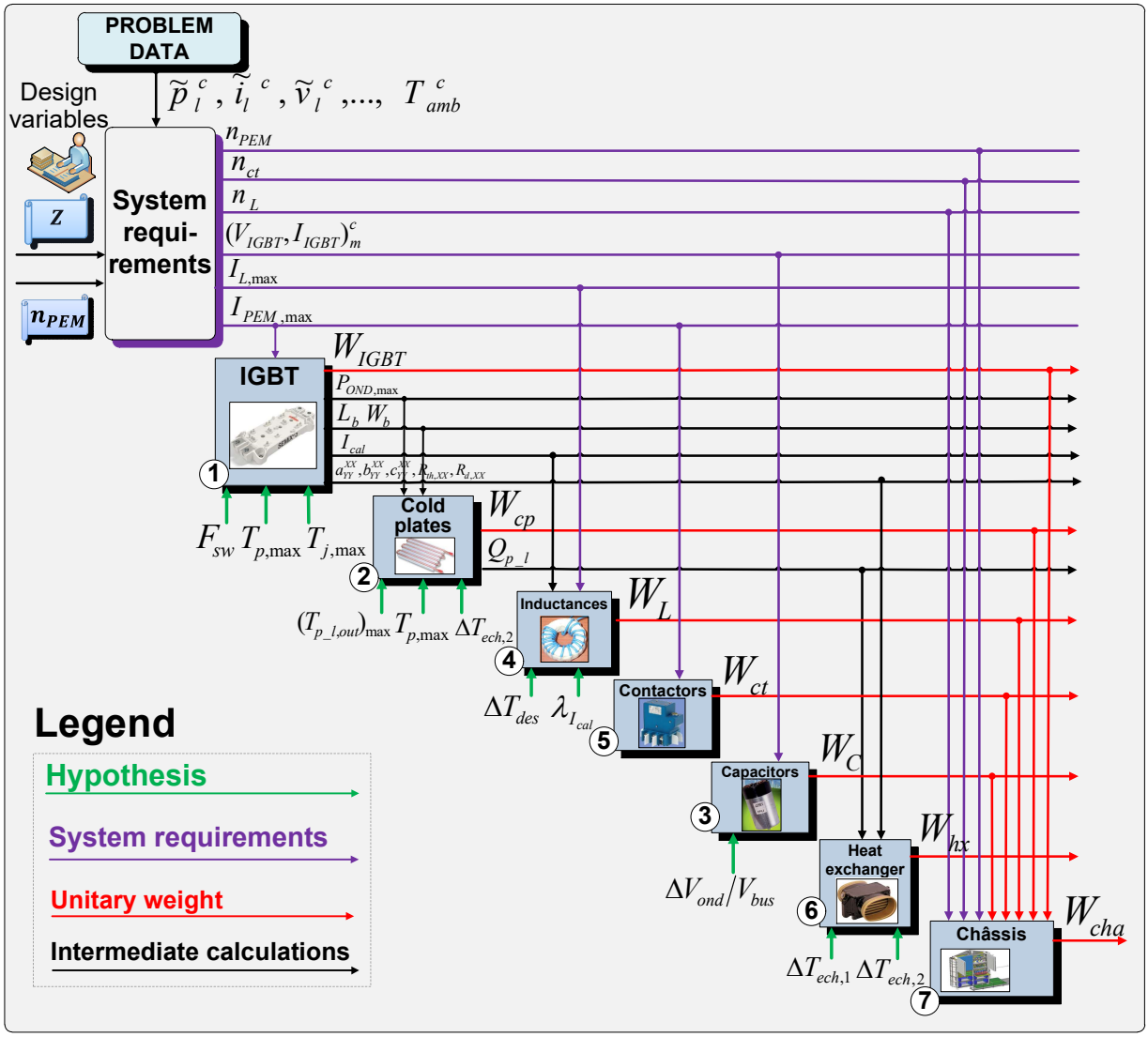

Figure 17 N2D of the sizing process

IV.2 Axis 2 : sizing models

IV.2.1 Estimation models: state of the art

The sizing models represented here by different blocks are mainly formed by estimation models. As displayed on the Figure 18 these models aim to define secondary characteristics (e.g weight of an electromechanical actuator) according to primary characteristics (e.g rated torque) [22].

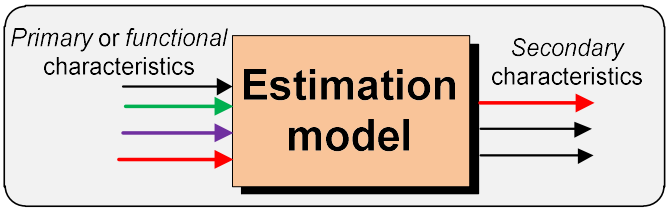

Figure 18 Input/output of an estimation model

Different techniques can be applied in order to link primary and secondary characteristics:

- **Component catalogue database**. The classical and easiest way is to use databases. For example, large IGBT module database with searching filters can be used online in order to select the components fulfilling the requirements (e.g voltage and current rating) [23]. Nevertheless if the number of product references is too low this technique is not suitable. This is particularly the case in the aerospace field for which the components are often designed for a particular application.
- **Detailed design models** consist in designing the whole component: choosing the geometrical dimensions, the type of material, etc. The complexity depends on the study context : from a simple routine made of analytical equations to a model made of numerical simulations coupled with optimization algorithms [24].
- **Scaling laws** (also called similarity models) study the effects of varying representative parameters of a component compared with a known reference. This technique is used in different physical fields : electrical [25] [26], electro-mechanical [27] [28], thermal [29].
- **Meta models and response surface approximations** (also called surrogate models) is a mathematical method enabling to model analytically a phenomena or a system according to a limited number of references. The response surface approach is often used in order to obtain a polynomial equation modelling directly a complex system. This technique is widely spread in different engineering fields : electrical [31], automatics [32], electro-mechanical [33].

IV.2.2 Summary of the different techniques in the sizing process

The Table 1 provides an outlook of the different techniques employed for the estimation models necessary for our case study. For some components such as the IGBT modules and the inductances, several techniques are required in order to build the estimation models.

	Database	**Detailed design model**	**Scaling laws**	**Response surface**
1) IGBT modules	X		X	X
2) Cold plates		X		
3) Capacitors	X			X
4) Inductances	X	X	X	X
5) Contactors	X			
6) Heat exchanger		X		
7) Chassis				X

Table 1 Summary of the different estimation model techniques used in the sizing process

IV.2.1 Sizing model example : the inductances

The estimation model of the inductance is a good example representative of the techniques employed in order to obtain accurate and rapid sizing blocks.

IV.2.1.1 Detailed design

In a first step, a detailed design model is defined in order to derive the geometrical dimensions of a toroidal shape mono-phase inductance as displayed in Figure 19. A computation routine is developed; it is based on 4 items:

- Item 1: 8 high level parameters (Table 2): the self-inductance value, the inductance peak current, etc. These parameters are given by the routine user;

- Item 2: a set of geometrical relationships derived by approach mixing scaling laws and the use of industrial database [34] [35];
- Item 3: a set of physical relationships modelling the inductance (magnetics and thermal fields). These equations form the physical model;
- Item 4: 2 design variables defined in the Table 3.

These 2 design variables are processed by a solver in order to find a feasible solution of the problem according to the data specified by the item 1, 2 and 3. The running time for solving the problem is around 1 second.

IV.2.1.2 Response surface

In a second step, the response surface technique is used. Several runs of the detailed design model are here necessary before to enable finding an analytical relationship linking the weight « W_L », the peak current « I_L » and the self-inductance value « L »:

$$W_L = 1.45.10^{-4}.L^{0.85}.{I_L}^{1.68} \qquad Eq.\ 8$$

with the following unit choices: « $W_L : kg$ » ; « $L : \mu H$ » ; « $I_L : A$ ».

By using the *Eq.8* instead of running directly the detailed design model, the weight of the inductance can be determined nearly "instantaneously" in comparison with the 1 second range of the solver. A significant computation time gain is reached.

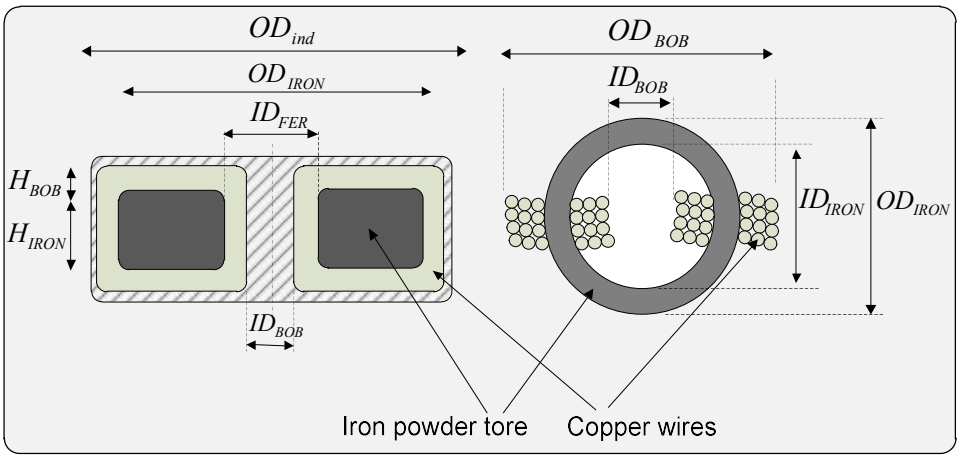

Figure 19 Geometrical dimensions of a toroidal shape mono-phase inductance

Parameter definition	Notation		Parameter definition	Notation
Self-inductance value	« L »		Electrical frequency	« F_{mod} »
Inductance peak current	« I_L »		Relative current ripple	« $\Delta I_L/I_L$ »
Bus voltage	« V_{bus} »		Ambient temperature	« T_{amb} »
Switching frequency	« F_{sw} »		Thermal convection coefficient	« h »

Table 2 High level parameter of the detailed design model of the inductance

Design variables	Value range	Notation
Maximal induction in the tore	$[0\ ;0.5]\ Tesla$	« B_{max} »
Winding fill factor	$[0\ ;0.5]$	« K_u »

Table 3 Design variables of the detailed design model of the inductance

V. Optimization algorithm: a dedicated heuristic

Exact methods such as the branch and bound algorithm [36] cannot be applied due to the size of the problem (combinatorial explosion). For the same reason, meta-heuristics (Tabu search [37], Simulated annealing [38], etc) usually use in combinatorial optimization problems are inefficient. Therefore a dedicated algorithm is developed for the IMPEC optimal design problem. This algorithm uses the evaluation function introduced here before each time a system weight assessment is required.

V.1 Presentation of the heuristic algorithm

As illustrated by the Figure 21, the heuristic is made of 2 successive steps.

V.1.1 Step n°1 : data preparation

The step 1 consists in a pre-processing computation enabling to define several physical features of the system for different PEM current levels « $I_{PEM,max}$ ». This current is the maximum current level seen by the PEM semi-conductors over all the loading cases « $\mathcal{C}$ ». The value of « $I_{PEM,max}$ » represent the PEM nominal power. The step 1 is decomposed as follows:

- **Step 1.A** determines the different values of « $I_{PEM,max}$ » for the complete design problem. There is a discrete number of possible « $I_{PEM,max}$ » values since the load current is "produced and distributed" by a discrete number of PEMs.
- **Step 1.B** identifies, for each « $I_{PEM,max}$ » value, a set of physical features required by the design solution: the minimal number of PEMs « $n_{PEM,min}$ », the minimal number of inductances « $n_{L,min}$ » and the minimal contactor matrix « MAT_{min} ». This matrix contains the minimal number of contactors « $n_{ct,min}$ » required not to exceed « $I_{PEM,max}$ » at PEM level. The Figure 20 provides an example of the information type delivered as outputs by the end of step 1.B. The example shows that for a PEM commuting a maximum current of « $100\ A$ », the IMPEC solution requires at least 5 PEMs and the contactor matrix needs to embed 14 contactors.

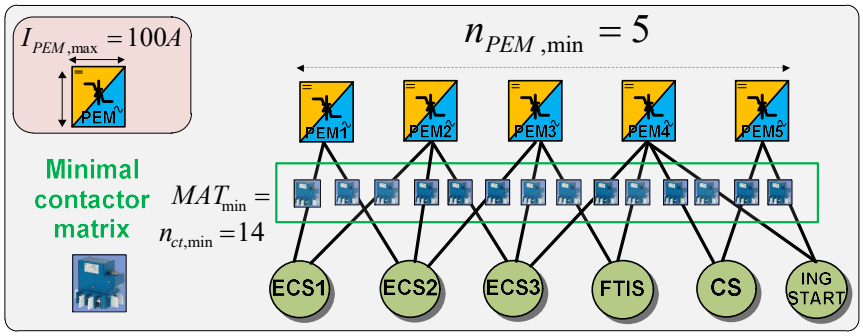

Figure 20 Example of the minimal number of PEMs & minimal contactor matrix for « $I_{PEM,max} = 100\ A$ »

All these data will be used as inputs for the heuristic step 2. These physical characteristics and in particular the contactor matrix definition enable to drastically reduce the

combinatorial space for the definition of the reconfiguration solution « Z » (connexion of load/PEM for all the loading cases) without excluding the most promising solutions.

V.1.2 Step n°2 : optimization

The step 2 is the core part of the optimization algorithm. It defines the design variables « $z_{l,m}^{c}$ » forming the reconfiguration solution « Z ». From a value of « $I_{PEM,max}$ » and for the associated set of physical features, the step 2 is made of 2 successive steps:

- **Step 2.A** intends to build a solution having the *minimal number of contactors* « $n_{ct,min}$ » by using the minimal contactor matrix « MAT_{min} ». For each loading case « c », a matrix configuration is found by the greedy algorithm in order to minimize the system weight « W_S » as specified in the part III.1.2. The greedy algorithm is a typical method used in combinatorial optimization [39]. The simplicity and rapidity of this algorithm enables to cope with the combinatorial explosion for the choice of the reconfiguration solution. This is qualified as a *construction* algorithm since the solution is built at each step of the process. In our application, it means that at each step of the algorithm, the matrix configuration of one loading case is decided. This choice is not re-challenged during the rest of the exploration of the greedy algorithm.

  The Figure 22 shows the type of outcome that could produce the greedy algorithm on a simple problem made of 4 loading cases, 2 PEMs and 3 loads. In this illustrative problem the minimal contactor matrix « MAT_{min} » is given on the left-hand side of the Figure 22. The PEM is rated as « $I_{PEM,max} = 30\ A$ ». The first step of the method consists in assessing the 3 different configurations for the loading case n°1. The configuration leading to minimum weight is taken. Here it is the configuration n°2. This choice will not be re-challenged in the greedy algorithm process. Then the second iteration of the algorithm goes to the case n°2 for which there is only one choice due to « MAT_{min} » and the loads' power demand. The same situation appears for the loading case n°3. Then the algorithm finishes with the loading case n°4 for which there are again 3 different configurations. The choice n°3 is taken since it minimizes the weight.

  The greedy algorithm ends up with the solution « $s1 = (\theta 1, Z1)$ » (see Figure 21) . On our illustrative example, the solution « $s1$ » has a weight of 81 kg. The matrix reconfiguration solution « $Z1$ » consists of the configuration highlighted in red on the Figure 22. The physical constitution « $\theta 1$ » of the solution « $s1$ » is 3 PEMs, 4 contactors and 3 inductances (one at each PEM output – since each PEM is parallelized during the loading case n°2 and n°3).

  If the solution « $s1$ » has the minimum number of inductances « $n_{L,min}$ », the step 2 is over. Otherwise the step 2.B is launched. In our illustrative example, the minimum number of inductances is « $n_{L,min} = 2$ » therefore the step 2.B shall be launched.

- **Step 2.B** intends to modify locally « $s1$ » in order to obtain a solution having *a minimal number of inductances*. Only loading cases implying PEM paralleling are modified in order to delete one or several inductances. During this step, several solutions « sj » (with « $j \geq 2$ ») can be produced. They are the trade-off between solutions having a minimal number of inductances « $n_{L,min}$ » and those having a minimal number of contactors « $n_{ct,min}$ ».

  In the illustrative example, a possible modification brought by the step 2.B would have been to modify the configuration of the loading case n°3 as illustrated on the Figure 23. The load n°1 is now connected to the PEM3 and the load n°2 is supplied by PEM1 and PEM2. If it is the only modification brought to « $Z1$ », the new matrix reconfiguration solution « $Z2$ » will lead to delete the inductance

at the output of PEM n°3. The minimal number of inductances is reached. On the other hand, 2 new contactors are required in comparison to « MAT_{min} » : one contactor between PEM1 and load n°2; one contactor between PEM3 and load n°1. The physical constitution « $\theta 2$ » of the new solution « $s2$ » is 3 PEMs, 6 contactors and 2 inductances.

When the step 2 is over, a new value of « $I_{PEM,max}$ » is taken. All along the algorithm run, the produced solutions are stored (right-side block on the Figure 21). The solution having the most performing weight value « $\widehat{W}_{s,HEUR}$ » is extracted.

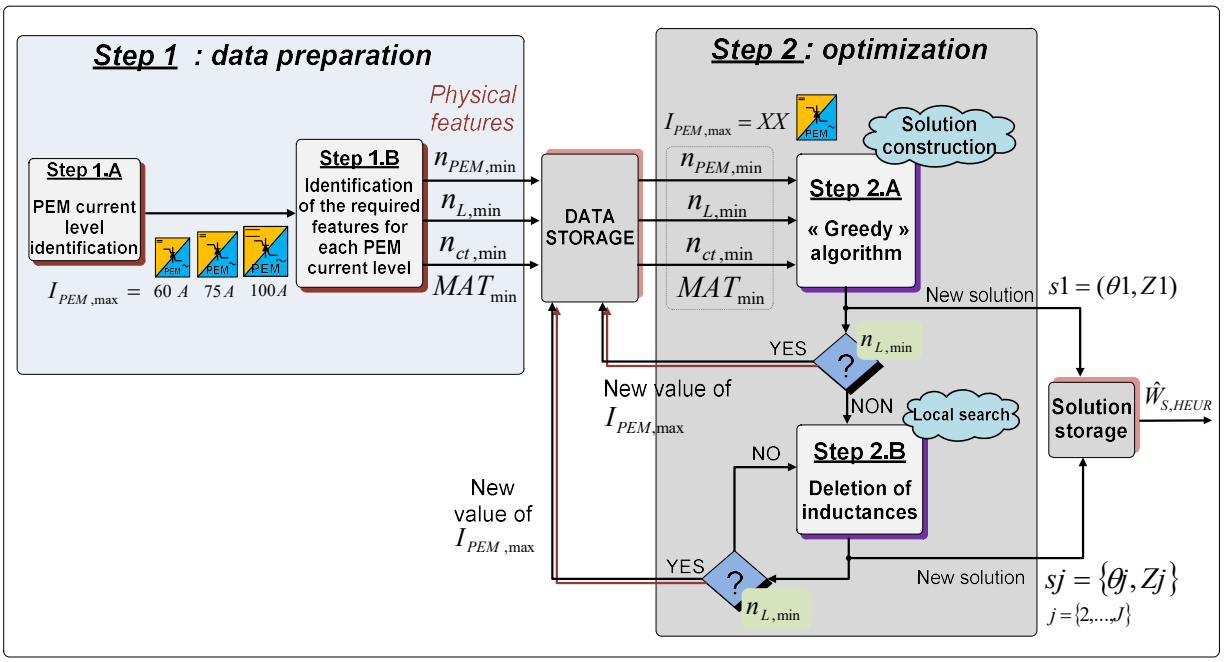

Figure 21 General algorithm of the 2-step heuristic

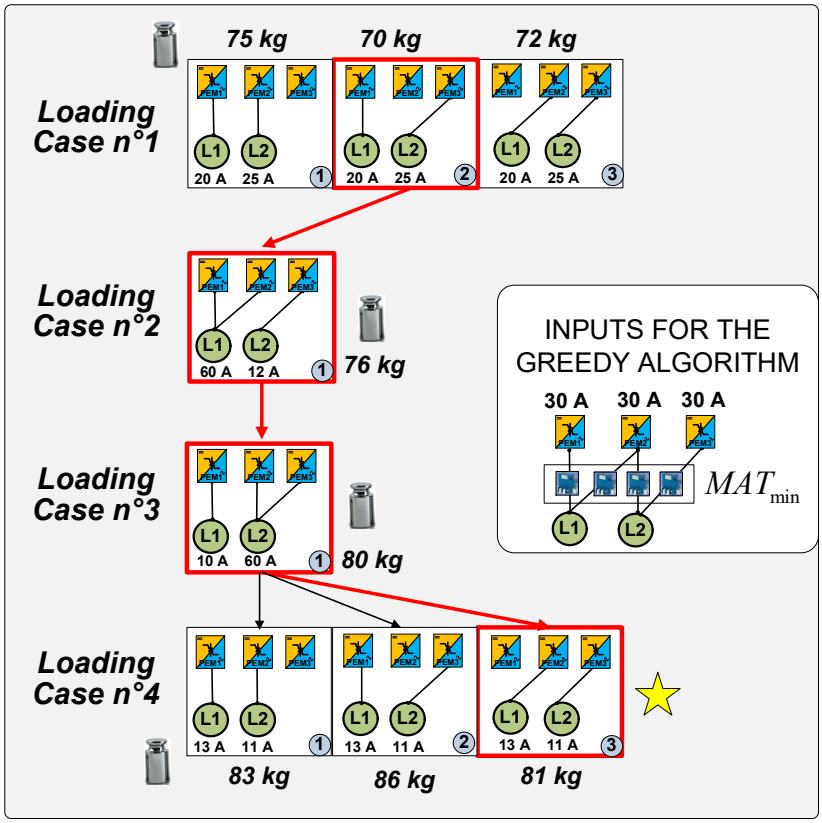

Figure 22 Step 2.A : Outcome of a greedy algorithm on problem made of 3 PEMs, 2 loads for a given minimal contactor matrix

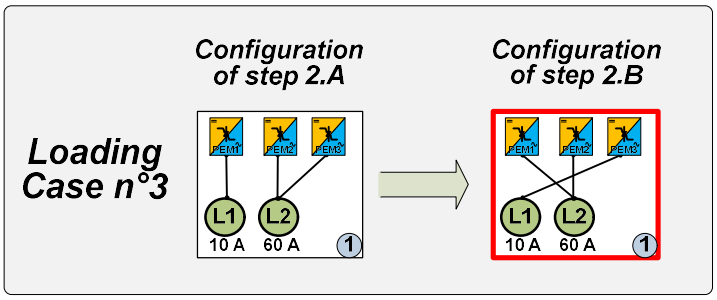

Figure 23 Possible local modification carried out by the step 2.B

V.2 Heuristic results form

V.2.1 At the end of the step 1

The algorithm step 1 was applied on the industrial use case studied in this paper (part II.3). On a *Quad Core 2.67 GHz* machine, it takes around 1 hour to carry out the step 1.

The results are displayed on the Figure 24 indicating the 3 main features computed by this data preparation step: « $n_{PEM,min}$ », « $n_{ct,min}$ », « $n_{L,min}$ » according to the 160 different values of « $I_{PEM,max}$ » for the industrial use case.

For each « $I_{PEM,max}$ » value, 3 different points representing the 3 main features are plotted. For a solution having the highest « $I_{PEM,max}$ » value, the data given by the step 1 are : « $n_{PEM,min} = 5$ », « $n_{ct,min} = 14$ », « $n_{L,min} = 0$ » (PEM paralleling is not possible).

If these 3 numbers are seen as an image of the solution physical complexity, thus the Figure 24 shows that the « $I_{PEM,max}$ » decrease implies the increase of the solution complexity.

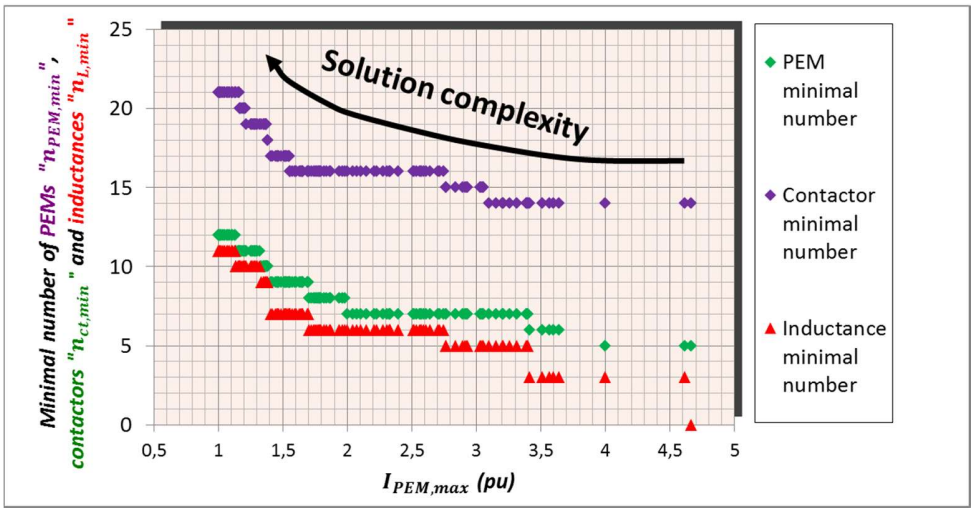

Figure 24 Evolution of the minimal number of PEMs, contactors and inductances

V.2.2 At the end of the step 2

At the end of the step 2, a complete set of solutions is stored (right-side block on the Figure 21). The Figure 25 shows the performance of these solutions according to the PEM size (the current « $I_{PEM,max}$ ») for typical component technologies. A classification based on the number of PEM is displayed: from « $n_{PEM} = 5$ » to « $n_{PEM} = 12$ ». These results are obtained for the industrial use case (part II.3). On a *Quad Core 2.67 GHz* machine, the optimization process lasts around 12 hours in order to compute all the solutions displayed on the Figure 25.

The Figure 25 highlights the *solution set X* regrouping all solutions found by the algorithm that have 6 PEMs and « $I_{PEM,max} = 3.4\ pu$ ». This *solution set X* is the output of a single iteration of the step 2. As shown on the top right corner of the Figure 25, it is made of 4 solutions having different characteristics in terms of « n_{ct} » and « n_L ». The most performing solution of the *solution set X* is the one having the minimal

number of contactors: « $n_{ct} = 14$ » and « $n_L = 4$ ». No solution having simultaneously the minimal number of contactors and the minimal number of inductances was found.

The Figure 25 highlights 3 particular solutions. On the right-hand side, the *least complex solution* weights « $1.17\ pu$ » and is made of only 5 PEMs commuting a current of « $I_{PEM,max} = 4.65\ pu$ ». The *most performing solution* (or optimal solution for the algorithm) is made of 8 PEMs with « $I_{PEM,max} = 1.75\ pu$ ». On left-hand side, the *most complex solution* is made of 12 small PEMs with an increased weight of « $1.14\ pu$ ». Additionally, it is interesting to notice that even though the *least complex* and *most complex* solutions have very different physical constitutions, their weight are nearly similar.

Except for the class with minimal number of PEMs (i.e. 5 in this example), Further analysis of solutions displayed on the Figure 25 shows that, given a class of solutions (i.e. set of solutions having the number of PEM), the best one is provided by minimizing « $I_{PEM,max}$ ». For example among the class of solutions having 7 PEMs, the lightest solution is the one having the minimal PEM power: « $I_{PEM,max} = 2.0\ pu$ ».

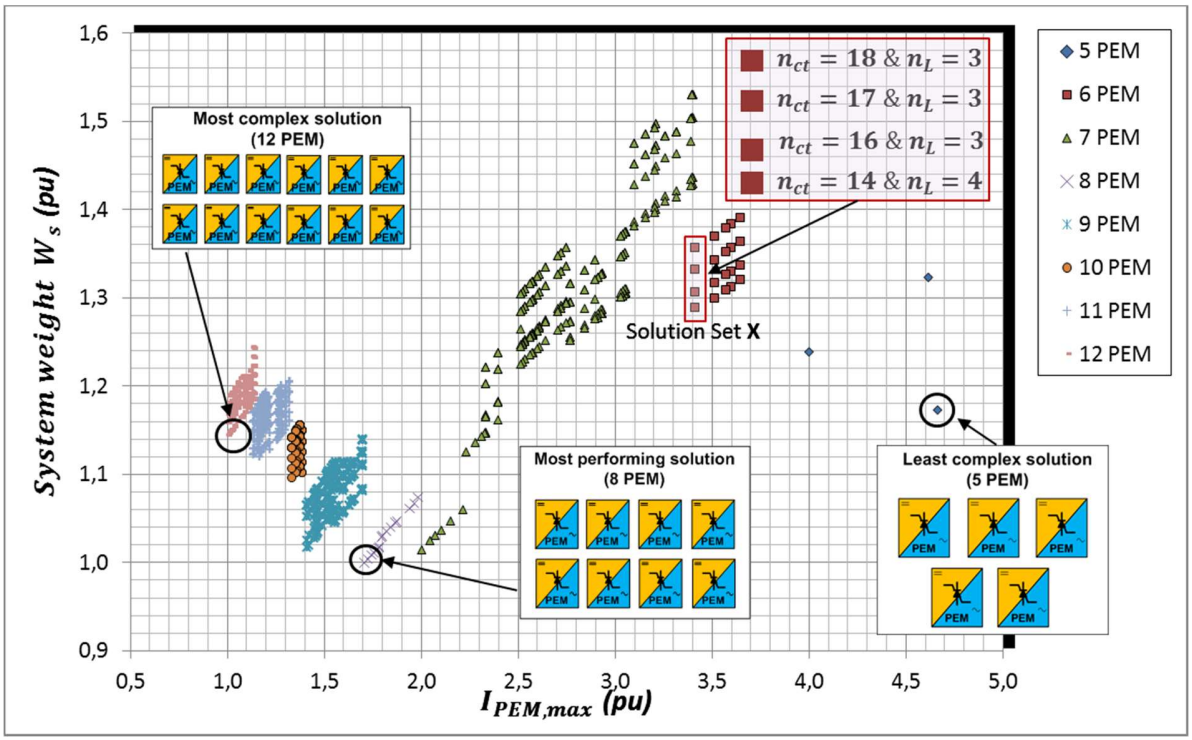

Figure 25 Performance of the solutions produced by the heuristic

V.3 Validation of the heuristic performance

The performance of the dedicated algorithm was assessed through 3 different types of problems with different size:

- On 16 *reduced-size problems* with a limited number of loading cases (around 40) , loads (3) and PEMs (up to 7), the problems can be exactly solved by the Branch and Bound algorithm [36]. Although the problems can be qualified as “reduced-size”, the combinatorial space can go up to « $\approx 10^{112}$ » solutions.

The performance assessments show that the heuristic is capable to find the optimal solution for nearly all the problems (except one). The heuristic computation time is extremely fast (several seconds) whereas the Branch and Bound can take up to 5 hours to find the optimal solution.

- On *industrial problems* presented in the part II.3 but with a limited number of PEMs (up to 7), a lower bound values can be identified (a dedicated algorithm, not explained in this paper, was developed in order to find a lower bound value).

  The assessments show that the heuristic is on average at 6 % of the lower bound. This means that in the most unfavorable situation, the heuristic produces a solution 6 % away from the optimum.

- On *industrial problems* presented in the part II.3 with a number of PEMs going from 5 to 12. A reference solution is defined by applying the rules of thumb usually applied on the industrial field. The assessments show that the heuristic is capable to find on average a solution offering 25 % weight savings according to the reference solution.

VI. Post-optimal analysis

VI.1 Identification of the most robust solution class

On the industrial problem used for our study, the heuristic defines 160 values of « $I_{PEM,max}$ ». That is to say 160 solution forms, defined by the couple « $I_{PEM,max}$; n_{PEM} », are produced by the optimization algorithm. As already shown by the Figure 25, for typical component technologies, the heuristic shows that the most performing solution is offered with « $I_{PEM,max} = 1.75$; $n_{PEM} = 8$ ».

As technologies are evolving rapidly and as there are always uncertainties on the sizing models, cartography is carried out by solving the problem with different combinations of component characteristics:

- the IGBT power losses ;
- the inductance weight ;
- the contactor weight ;
- the capacitor weight.

In addition, 3 levels (low, nominal & high) are defined for each component characteristic. For instance, if the "nominal" value of the contactor weight characteristics is « $200\ Amp/kg$ ». The "low" (pessimistic performance view) and "high" (optimistic performance view) values are respectively « $100\ Amp/kg$ » and « $300\ Amp/kg$ ».

In total, 81 (3^4) combinations are set. In order to have a synthetic view over these 81 runs, the Figure 26 is built. On each graph, the 160 solution classes are displayed.

The upper part of the graph shows for each solution class the mean difference to the optimal solution. For instance, the solution class n°53 defined by the couple: « $I_{PEM,max} = 2$; $n_{PEM} = 7$ » is on average at 5 % of the optimal solution for the 81 component characteristic combinations. The lower part of graph of the Figure 26 shows the standard deviation to the optimal solution. Both graphs clearly show that the most robust solution classes are between « $n_{PEM} = 7$ » and « $n_{PEM} = 9$ » with a PEM power between « $I_{PEM,max} = 1.4\ pu$ » and « $I_{PEM,max} = 2\ pu$ ».

Finally, it is interesting to notice that over the 81 runs, only 4 solution classes are optimal. They are highlighted in red color (the number of times in which they are optimal is written just below). Thus the solution class n°1 defined by the couple: « $I_{PEM,max} = 4.7$; $n_{PEM} = 5$ » is the best solution for 17 out of 81 runs (combination of component characteristics).

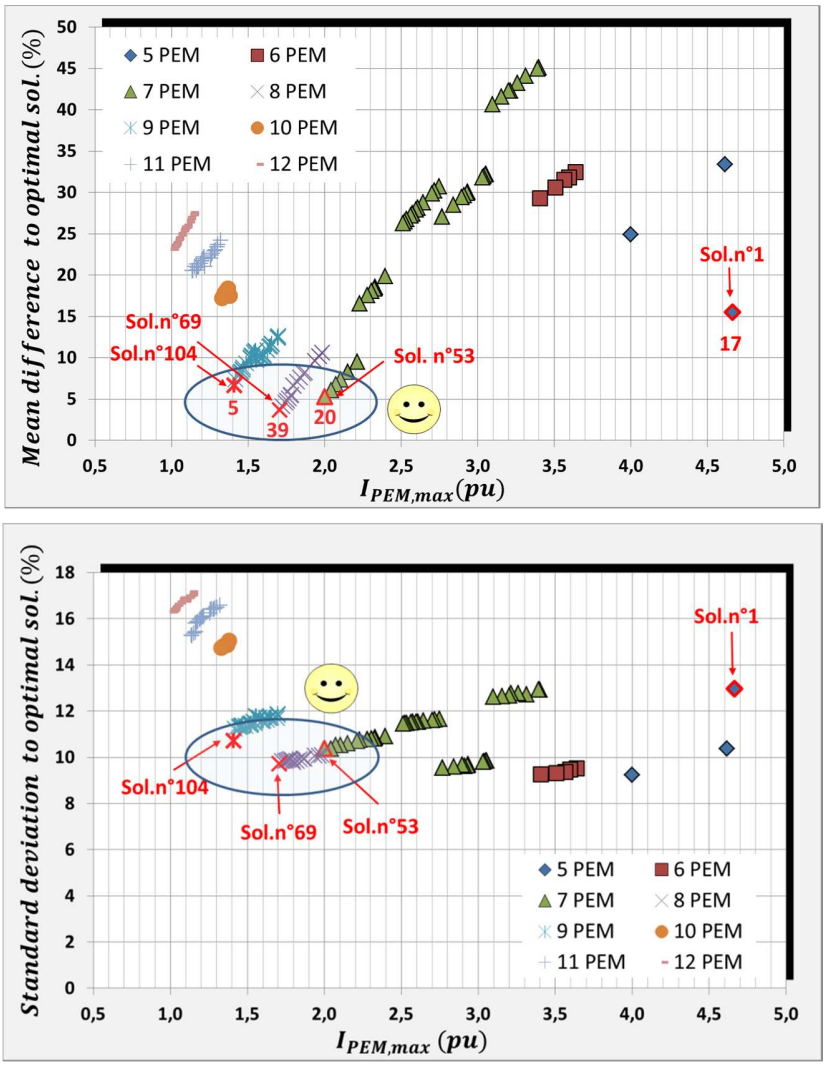

Figure 26 For 81 solution performance combinations – Upper part : the mean difference to the optimal solution – Lower part: standard deviation to optimal solution.

VI.2 Solution sensibilities

By exploiting the previous 81 runs, a design of experiments (DOE) is carried out over the 4 solution classes mentioned previously. This DOE enables to quantify the sensibilities of the 4 solution classes according to previous 4 component characteristics: IGBT power losses, inductance weight, contactor weight, capacitor weight.

The linear effects of the different component characteristics over the overall system weight are identified. The results of this DOE are displayed on the Figure 27. It is clearly shown that the contactors and inductances are the most influencing elements over the overall system weight. For instance, on the 4 solution classes: the contactor weight effect is 3 times higher than the capacitor weight effect.

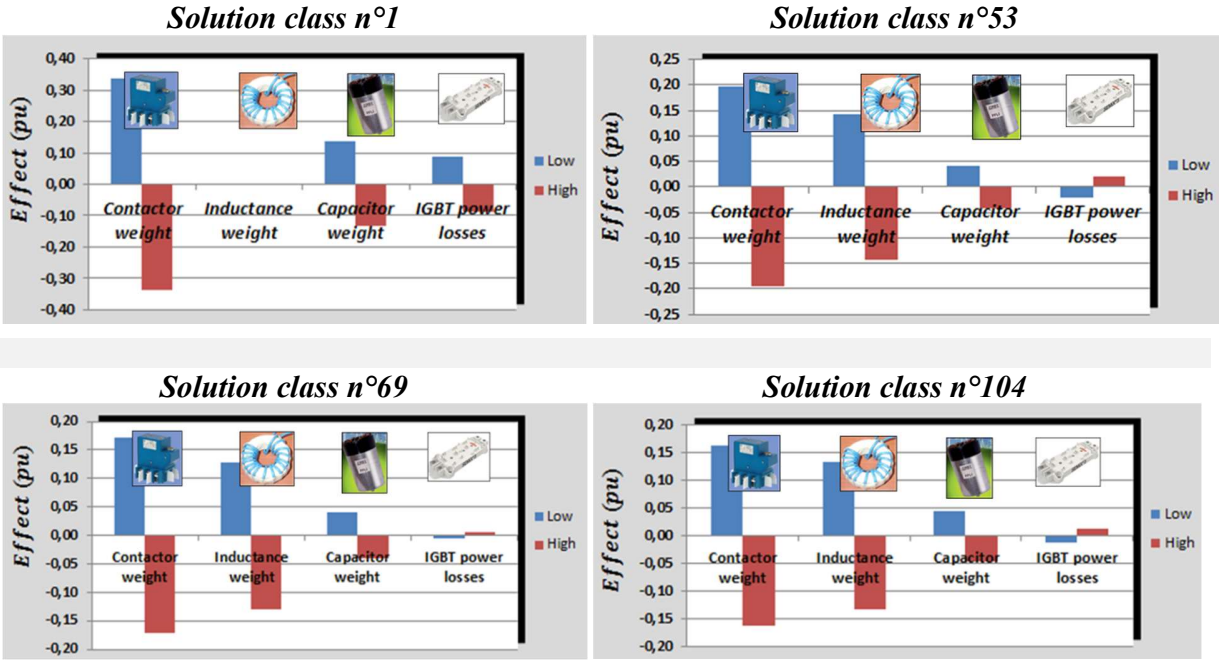

Figure 27 Results of the DOE on the most robust and performing solutions

VII. Conclusion

Today the More Electrical Aircraft (MEA) trend is transforming step by step the aeronautical field. Among several technological bricks required for the MEA, power electronics is one of the most important technologies. With MEA, more and more power electronics modules need to supply high power systems consuming up to 100 kW (e.g the Environmental Control System called ECS). This significant change in terms of power demand requires to design innovate concepts for supplying of electrical loads requiring power electronic interfaces.

Traditionally aircraft loads requiring power electronics are supplied by a dedicated power electronics module (PEM). For such a structure, this paper has highlighted several drawbacks: reliability aspect (the PEM loss implies the load loss), cost aspect (the number of PEM references is equivalent to the load number), the PEM low utilization rate (if the load is intermittent). The Integrated Modular Power Electronic Cabinet (IMPEC) has been designed to tackle these drawbacks. IMPEC can be seen as the *power electronics* twin of the well-known IMA (Integrated Modular Avionics) that is the current embedded solution for *processing electronics (28V DC)*.

IMPEC is made of several identical (modular) PEMs that can supply a set of electrical loads. A load can be supplied by one or several PEMs at a time. A matrix contactor enables to make the association « PEM-load ». IMPEC offers flexibility to the operational needs by changing the association « PEM-load » from one operational case to another one.

In this context, the present paper has described a methodology for the IMPEC optimal design. To our knowledge, this is the first time that a complete design methodology is developed for such a system. As often in aeronautical applications, the design objective consists in minimizing the overall system weight. In addition, two design variables can be processed by the optimization algorithm: the number of PEMs and the reconfiguration of the contactor matrix. The characterization of the optimal design problem highlighted two main features: the multi-physical system sizing and the combinatorial explosion mainly due to the contactor matrix reconfiguration. The mixing of these two issues within a same problem is not usual and forms a complex problematic requiring innovative approaches.

Since designer shall cope with a combinatorial explosion, an explicit and rapid sizing process was developed. The process was cut into several sizing blocks: one for each component type. By introducing design hypothesis, all loops were deleted between the different sizing blocks. Within each sizing block, simple relations such as analytical equations were used. These equations can have been established beforehand by using high demanding processing methods such as solvers or simulations.

Since the classical combinatorial optimization algorithms were not sufficiently efficient due to the problem size, a dedicated method was developed. This heuristic was made of 2 steps: 1) pre-processing enabling to define beforehand a set of physical features of the solutions (PEM number, contactor number, inductance number) 2) the successive launch of a greedy algorithm and a local search algorithm in order to define the contactor matrix reconfiguration. The performance of this innovative algorithm was validated on problems of different sizes. In particular, the heuristic was capable to detect the optimal solution nearly instantaneously on *reduced-size* problems whereas several hours can have been required for a branch and bound algorithm.

Additionally, the complete heuristic results showed that - except for the minimal number of PEM - within a set of solutions having the same number of PEMs, the lightest solution is the one minimizing the PEM power. In the future, this observation could be employed in order to speed up the detection of the more promising solutions.

The complete methodology introduced in this paper was employed to identify the most robust classes of solutions according to different technology characteristics: IGBT power losses level; weight of contactors, inductances and capacitors. The study showed that only 4 solution classes were optimal among 160 created by the heuristic. A design of experiments, applied on these 4 solution classes, quantified their linear sensibilities according to the technology characteristics. The results have highlighted that the weight of contactors and inductances were clearly the main drivers enabling to bring weight savings in the future. Eventually, the optimization of the component sizing (in particular these commutation components) is the main perspective of this work.

References

[1] I. Moir, A. Seabridge, *Aircraft Systems – Mechanical, electrical, and avionics subsystems integration*, Third Edition, Wiley, 2008.

[2] S. Liscouët-Hanke, *A model-based methodology for integrated preliminary sizing and analysis of aircraft power system architectures*, PhD Thesis, INSA Toulouse, 2008.

[3] J.A. Rosero, J.A. Ortega, E. Aldabas, L. Romeral, *Moving towards a more electrical aircraft*, IEEE Aerospace Electrical Systems, vol.22, n.3, pp. 3-9, 2007.

[4] X. Roboam, *New trends and challenges of electrical networks embedded in "more electrical aircraft"*, IEEE International Symposium on Industrial Electronics, pp 26-31, 27-30, June 2011.

[5] X. Roboam, B. Sareni, A. De Andrade *"More electricity in the air: Towards optimized electrical networks embedded in "more electrical aircraft",* IEEE IEM (Industrial Electronics Magazine), Vol 6, issue IV, pp 6-17, December 2012

[6] Mike Sinnett, "*787 No-Bleed Systems:* Saving Fuel and Enhancing Operational efficiencies", Boeing, Aero Magazine, QTR_4.07 http://www.boeing.com/commercial/aeromagazine

[7] M. Todeschi, Airbus - *EMA's for flight controls actuation systems - 2012 status and perspectives, perspectives*, International conference on Recent Advances in Aerospace Actuation Systems and Components, June 13-14, 2012, Toulouse, France.

[8] Olaf Cochoy, Susan Hanke, Udo B. Carl, *Concepts for position and load control for hybrid actuation in primary flight controls*, Aerospace Science and Technology, Volume 11, Issues 2–3, March–April 2007.

[9] D. Van den Bossche, *A380 primary flight control actuation system*, International conference on Recent Advances in Aerospace Actuation Systems and Components, June 13-15, 2001, Toulouse, France.

[10] European research project "*CleanSky*" : www.cleansky.eu

[11] European research project "*Actuation 2015*" : http://www.actuation2015.eu/

[12] L. Prisse, D. Ferer, H. Foch, A. Lacoste, *New power centre and power electronics sharing in aircraft*, EPE Barcelone, 2009.

[13] J.W Ramsey, *Integrated Modular Avionics : Less is More*, Avionics Today, 2007.

[14] P.J Prisaznuk, *Integrated modular avionics*, Aerospace and Electronics Conference, 1992. Proceedings of the IEEE 1992 National , vol., no., pp.39,45 vol.1, 18-22 May 1992.

[15] X. Giraud, M. Sartor, X. Roboam, B. Sareni, H. Piquet, M. Budinger, S. Vial, *Load allocation problem for optimal design of aircraft electrical power*, International Journal of Applied Electromagnetics and Mechanics (IJAEM), Volume 43, Number 1-2, pp. 37-49, 2013.

[16] B. Annighofer, E. Kleemann, & F. Thielecke. *Automated selection, sizing, and mapping of Integrated Modular Avionics Modules*, In Digital Avionics Systems Conference (DASC), 2013 IEEE/AIAA 32nd (pp. 2E2-1). IEEE.

[17] S. Liscouet-Hanke, K. Huynh, *A Methodology for Systems Integration in Aircraft Conceptual Design – Estimation of Required Space*, SAE 2013.

[18] B. Delinchant, F. Wurtz, D. Magot, L. Gerbaud, *A Component-Based Framework for the Composition of Simulation Software Modeling Electrical System*, SIMULATION, Vol. 80, July/August 2004 80 : 347-356.

[19] NASA, *Techniques of Functional Analysis*, NASA Systems Engineering Handbook, 1995.

[20] Internet website: http://www.dsmweb.org

[21] T.R. Browning , *Applying the Design Structure Matrix to System Decomposition and Integration Problems:A Review and New Directions*, IEEE Transactions on Engineering Management, Vol. 48, no. 3, august 2001.

[22] M._Budinger, J._Liscouët, F._Hospital, J.C._Maré, *Estimation models for the preliminary design of electro-mechanical actuators,* Journal of Aerospace Engineering 226, 3, pp 243-259, 2012.

[23] SEMIKRON WEBSITE : http://www.semikron.com/products/product-classes/igbt-modules.html

[24] B. Sareni, L. Krähenbühl, D. Muller, *Niching Genetic Algorithms for Optimization in Electromagnetics, II. Shape Optimization of Electrodes using the CSM,* IEEE Trans. on Magnetics, Vol. 34, No. 5, pp. 2988-2991, 1998.

[25] A. De. Andrade, A. Lesage, B. Sareni, T. Meynard, X. Roboam, R. Ruelland, M. Couderc, *Integrated optimal design for power systems of more electrical aircraft*, Conference More Electric Aircraft, Bordeaux, 2012.

[26] F. Forest, E. Laboure, T.A. Meynard, and V. Smet, D*esign and Comparison of Inductors and Intercell Transformers for Filtering of PWM Inverter Output,*IEEE Transactions on power electronics, vol. 24, no. 3, March 2009.

[27] M._Budinger, J._Liscouët, F._Hospital, J.C._Maré, *Estimation models for the preliminary design of electro-mechanical actuators,* Journal of Aerospace Engineering 226, 3, pp 243-259, 2012.

[28] Y. Fefermann, S. A. Randi, S. Astier, X. Roboam, *Synthesis models of PM Brushless Motors for the design of complex and heterogeneous system*, EPE'01, Graz, Austria, September 2001.

[29] M. Budinger, I. Hazyuk, F. Sanchez, J-Ch. Maré, *Scaling-law-based metamodels for the sizing of actuation systems*, Recent Advances in Aerospace Actuation Systems and Components, April 2-3, 2014, Toulouse, France.

[30] M. Jufer, *Design and Losses - Scaling Law Approach*, in Nordic Research Symposium Energy Efficient Electric Motors and Drives, Skagen, Denmark, , pp. 21-25, 1996.

[31] S. Brisset, F. Gillon, S. Vivier, P. Brochet, *Optimization with experimental design : an approach using Taguchi's Methodology and Finite Element Simulations*, IEEE Trans on Magnetics. Vol.37, N°5, pages 3530-3533, 2001.

[32] J. Faucher, P.Maussion, *Response surface methodology for the tuning of fuzzy controller dedicated to boost rectifier with power factor correction*, IEEE-ISIE : International Symposium on Industrial Electronics, 2006.

[33] T. El Halabi, M. Budinger, J.C. Mare. *Optimal geometrical integration of electromechanical actuators*, Recent Advances in Aerospace Actuation Systems and Components, May 5-7 2010, Toulouse, France.

[34] F. Forest, E. Labouré, T. Meynard, and M. Arab, *Analytic design method based on homothetic shape of magnetic cores for high frequency transformers*, IEEE Trans. Power Electron., vol. 22, no. 5, pp. 2070–2080, September. 2007.

[35] MICROMETALS - 200C SERIES – *High Temperature Powder Core For Power Applications* – Issue C – Feb. 2007.

[36] J. Clausen, *Branch and Bound Algorithms – Principles and Examples*, 1999 http://janders.eecg.toronto.edu/1387/readings/b_and_b.pdf

[37] A. Hertz, *Tabu search for large scale timetabling problems*, European Journal of Operational Research, Volume 54, Issue 1, page 39-47, 1991.

[38] S. Kirkpatrick, C.D. Gelatt, M.P. Vecchi, *Optimization by Simulated Annealing*, Science, New Series, Vol.220, 1983, pp.671-680.

[39] C. Garcia-Martinez, F.J. Rodriguez, M. Lozano, *Tabu-enhanced iterated greedy algorithm: A case study in the quadratic multiple knapsack problem,* European Journal of Operational Research, Volume 232, Issue 3, 1 Feb. 2014, Pages 454-463.